Journal of Applied Mechanics and Technical Physics, Vol. 45, No. 1, pp. 142–151, 2004

ESTIMATION OF THE EFFECTIVE ABSORPTIVITY OF METALS FROM THE OBSERVATION OF THEIR MARTENSITIC RESTRUCTURING UNDER LASER RADIATION

A. A. Evtushenko,[1] **E. G. Ivanik,**[2]
K. Rożniakowski,[3] **and I. M. Dobryanskii**[4]

UDC 539.377

A new experimental method is proposed for determining the effective absorptivity of a metal under pulsed laser radiation. The method is based on solving an axisymmetric boundary-value heat-conduction problem for a half-space with the use of metallographically measured sizes of the polymorphic-transformation zone in the irradiated material. The method is tested on single-crystal cobalt and St. 45 *steel samples.*

Key words: *laser, temperature, absorptivity, metal hardening.*

Introduction. Determination of the reflectivity R (or absorptivity $A = 1 - R$) of metals exposed to pulsed concentrated heat fluxes is a complicated problem that involves many factors, including the intensity of the incident laser radiation, space–time characteristics of the radiation pulses, wavelength of the electromagnetic wave, physical characteristics of the material (primarily, its chemical composition), metal surface finish, and properties of the ambient medium [1–3]. Normally, such measurements are performed by calorimetric methods, whose accuracy is generally low. Moreover, it should be taken into account that reflected radiation contains a diffusive component, whose registration requires the use of specially tailored calorimeters with wide fields of vision and high absorptivity [4–13].

At certain temperatures below the melting point, metals undergo polymorphic transformations or restructuring (recrystallization, growth of grains, etc.); as a result, a new crystalline structure is formed. In particular, at high cooling rates, there emerges the so-called martensite structure, whose dominating component is martensite, an oversaturated solution of carbon in α-iron. Regions with the martensite structure display enhanced hardness and high resistance to wear; these properties of the martensite structure are used in fabricating surface-hardened structural components for advanced machinery. In steels locally treated with laser radiation, the martensite-layer thickness can be rather accurately measured by metallographic methods with a scanning microscope [14–17].

The objective of the present study was to develop theoretical foundations and an experimental procedure for determining the effective absorptivity of metals, based on the analytical solution of an axisymmetric boundary-value heat-conduction problem for a semibounded body and measured sizes of the zone where structural transformations induced by laser radiation occur. The case of a one-dimensional (in terms of the spatial coordinate) temperature field was previously treated in [3, 18].

1. Formulation of the Problem. A laser beam acting on the surface of a metal with an incident light intensity of 10^4–10^8 W/m^2 is equivalent to a distributed source of heat of a certain specified power (heat flux with known intensity) [1]. Assuming that the laser power density is such that no material melting or evaporation occurs in the surface layer of the metal, the radiative and convective heat losses from the surface of the heated sample are

[1]Polytechnika Byalostotska, Byalystok, Poland. [2]Podstrigach Institute for Applied Problems in Mechanics and Mathematics, Ukrainian National Academy of Sciences, L'vov 79053, Ukraine. [3]Polytechnika Lodz'ka, Lodz' 93-590, Poland. [4]L'vov State Agricultural University, L'vov 80381, Ukraine. Translated from Prikladnaya Mekhanika i Tekhnicheskaya Fizika, Vol. 45, No. 1, pp. 173–184, January–February, 2004. Original article submitted March 25, 2003; revision submitted June 25, 2003.

 0021-8944/04/4501-0142

negligible, and all thermophysical characteristics of the material are temperature-independent, we formulate the following axisymmetric boundary-value heat-conduction problem for a semi-infinite body:

$$\frac{\partial^2 T}{\partial r^2} + \frac{1}{r}\frac{\partial T}{\partial r} + \frac{\partial^2 T}{\partial z^2} = \frac{1}{æ}\frac{\partial T}{\partial t}, \qquad r \geqslant 0, \quad z > 0, \quad t > 0; \tag{1}$$

$$T(r, z, 0) = 0, \qquad r \geqslant 0, \quad z \geqslant 0; \tag{2}$$

$$k\frac{\partial T}{\partial z} = -Aq(r)H(t_s - t), \qquad r \geqslant 0, \quad z = 0, \quad t > 0; \tag{3}$$

$$T(\infty, z, t) = T(r, \infty, t) = 0, \qquad t > 0. \tag{4}$$

Here T is the temperature, q is the radiation intensity, A is the effective (time-averaged integral) absorptivity, k is the thermal conductivity, $æ$ is the thermal diffusivity, r and z are the radial and axial coordinates in the cylindrical coordinate system whose origin coincides with the center of the heated spot, t is the time, t_s is the duration of the laser pulse, and H is the unit Heaviside function.

If the power density of incident radiation is uniformly distributed within the heating spot, which is a circle of radius a on the body surface, we have

$$q(r) = q_0 H(a - r), \qquad r \geqslant 0. \tag{5}$$

The power density of the incident radiation flux can also be represented as [19]

$$q(r) = q_f^* q^*(r), \qquad q^*(r) = [f + (1 - f)Kr^2]\exp(-Kr^2), \qquad r \geqslant 0, \tag{6}$$

where K is a coefficient that defines the sharpness of the heat-flux distribution peak, q_f^* is a certain characteristic value of the heat flux q, and $0 \leqslant f \leqslant 1$ is a parameter that characterizes the spatial distribution of the incident radiation intensity. Relation (6) yields the normal (Gaussian) distribution of the incident intensity for $f = 1$ and an annular distribution for $f = 0$.

Distributions (5) and (6) are related by the concentration coefficient K [1]:

$$K = B_f a^{-2}. \tag{7}$$

The numerical factor B_f in equality (7) can be found from the condition [3]

$$Q_f/Q = (1 - 1/e) \approx 0.632, \tag{8}$$

where, by virtue of (6),

$$Q = 2\pi \int_0^\infty q(r) r\, dr = \frac{q_f^*}{B_f}\pi a^2; \tag{9}$$

$$Q_f = 2\pi \int_0^a q(r) r\, dr = \{1 - [1 + (1 - f)B_f]\exp(-B_f)\}Q. \tag{10}$$

Substituting the total power density Q (9) and the power Q_f (10) concentrated within the circular region of radius a on the half-space surface into condition (8), we obtain the nonlinear equation for B_f

$$[1 + (1 - f)B_f]\exp(-B_f) = 1/e \approx 0.3678. \tag{11}$$

The roots B_f of Eq. (11) are linear functions of f: $B_f = B_0(1 - f) + f$ ($B_0 = 2.1462$ is the value of B_f for $f = 0$).

From condition (9), in addition to relations (5) and (6), we obtain

$$q_f^* = B_f q_0. \tag{12}$$

We introduce the following dimensionless variables and parameters:

$$\rho = \frac{r}{a}, \qquad Z = \frac{z}{a}, \qquad \mathrm{Fo} = \frac{æt}{a^2}, \qquad \mathrm{Fo}_s = \frac{æt_s}{a^2}, \qquad \Lambda = \frac{q_0 a}{k}. \tag{13}$$

Then, taking into account relation between (7), (12), and (13), we rewrite the boundary-value problem (1)–(4) as

$$\frac{\partial^2 T}{\partial \rho^2} + \frac{1}{\rho}\frac{\partial T}{\partial \rho} + \frac{\partial^2 T}{\partial Z^2} = \frac{\partial T}{\partial \mathrm{Fo}}, \qquad \rho \geqslant 0, \quad Z > 0, \quad \mathrm{Fo} > 0; \tag{14}$$

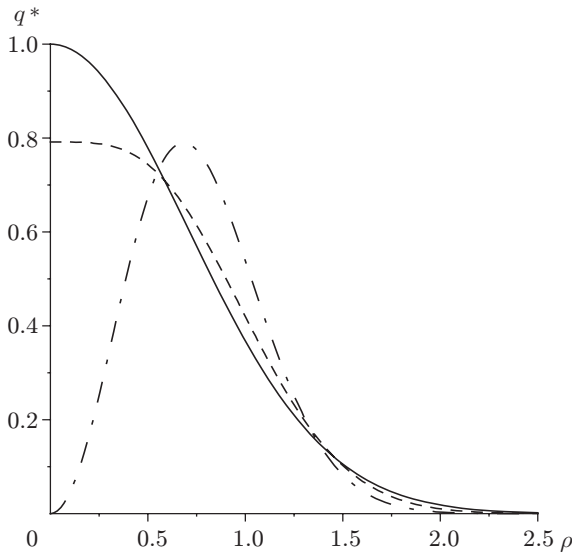

Fig. 1. Distribution of the dimensionless heat flux q^* (18) on the half-space surface.

$$T(\rho, Z, 0) = 0, \qquad \rho \geqslant 0, \quad Z \geqslant 0; \tag{15}$$

$$\frac{\partial T}{\partial Z} = -A\Lambda q^*(\rho) H(\mathrm{Fo}_s - \mathrm{Fo}), \qquad \rho \geqslant 0, \qquad Z = 0, \quad \mathrm{Fo} > 0; \tag{16}$$

$$T(\infty, Z, \mathrm{Fo}) = T(\rho, \infty, \mathrm{Fo}) = 0, \qquad \mathrm{Fo} > 0. \tag{17}$$

where

$$q^*(\rho) = B_f[f + (1-f)B_f\rho^2]\exp(-B_f\rho^2). \tag{18}$$

The function $q^*(\rho)$ given by formula (18) is plotted in Fig. 1 for three values of f. The solid, dashed, and dot-and-dashed curves in Figs. 1–7 refer to $f = 1$ [normal distribution of the radiation intensity (6)], $f = 0.5$, and $f = 0$, respectively.

2. Temperature Field. The solution of the boundary-value heat-conduction problem (14)–(17), obtained by successive application of integral zeroth-order Hankel transforms with respect to the radial variable r and the Laplace transform with respect to the time t, has the form

$$T(r, z, t) = A\Lambda \int_0^\infty \varphi(\xi)\Phi(\xi, Z, \mathrm{Fo}) J_0(\xi\rho)\, d\xi, \qquad r \geqslant 0, \quad z \geqslant 0, \quad t \geqslant 0; \tag{19}$$

$$\varphi(\xi) = b\int_0^\infty \rho q^*(\rho) J_0(\xi\rho)\, d\rho = \frac{1}{2}\Big[f + (1-f)\Big(1 - \frac{\xi^2}{4B_f}\Big)\Big]\exp\Big(-\frac{\xi^2}{4B_f}\Big), \qquad \xi \geqslant 0; \tag{20}$$

$$\Phi(\xi, Z, \mathrm{Fo}) = \Phi_0(\xi, Z, \mathrm{Fo}) H(\mathrm{Fo}) - \Phi_0(\xi, Z, \mathrm{Fo} - \mathrm{Fo}_s) H(\mathrm{Fo} - \mathrm{Fo}_s); \tag{21}$$

$$\Phi_0(\xi, Z, \mathrm{Fo}) = \frac{1}{2}\Big[\exp(-\xi Z)\,\mathrm{erfc}\Big(\frac{Z}{2\sqrt{\mathrm{Fo}}} - \xi\sqrt{\mathrm{Fo}}\Big) - \exp(\xi Z)\,\mathrm{erfc}\Big(\frac{Z}{2\sqrt{\mathrm{Fo}}} + \xi\sqrt{\mathrm{Fo}}\Big)\Big], \tag{22}$$

where J_m is the Bessel function of the first kind of order m and $\mathrm{erfc}(\cdot) = 1 - \mathrm{erf}(\cdot)$ [$\mathrm{erf}(\cdot)$ is the error function].

We consider some particular cases resulting from solution (19)–(22). As $t_s \to \infty$ ($\mathrm{Fo}_s \to \infty$), relation (21) yields $\Phi(\xi, Z, \mathrm{Fo}) = \Phi_0(\xi, Z, \mathrm{Fo})$, and expression (19) coincides with the solution for continuous emission [19, 20]. Passing to the limit in Eq. (22) as $t \to \infty$ ($\mathrm{Fo} \to \infty$), we obtain $\Phi_0(\xi, Z, \mathrm{Fo}) = \exp(-\xi Z)$, and solution (19) acquires the form

$$T(r, z, \infty) = A\Lambda \int_0^\infty \varphi(\xi)\exp(-\xi Z) J_0(\xi\rho)\, d\xi, \qquad r \geqslant 0, \quad z \geqslant 0. \tag{23}$$

Additionally putting $z = 0$ in Eq. (23), we find the stationary temperature on the half-space surface:

$$T(r, 0, \infty) = A\Lambda \int_0^\infty \varphi(\xi) J_0(\xi\rho)\, d\xi, \qquad r \geqslant 0. \tag{24}$$

Taking into account the form of the function $\varphi(\xi)$ (20) and the values of the integrals [21]

$$\int_0^\infty \exp\Big(-\frac{\xi^2}{4B_f}\Big) J_0(\xi\rho)\, d\xi = \sqrt{\pi B_f}\exp\Big(-\frac{B_f\rho^2}{2}\Big) I_0\Big(\frac{B_f\rho^2}{2}\Big),$$

$$\int_0^\infty \xi^2 \exp\Big(-\frac{\xi^2}{4B_f}\Big) J_0(\xi\rho)\, d\xi = \int_0^\infty \xi \exp\Big(-\frac{\xi^2}{4B_f}\Big) \frac{1}{\rho}\frac{\partial}{\partial\rho}\left[\rho J_1(\xi\rho)\right] d\xi$$

$$= \frac{1}{\rho}\frac{\partial}{\partial\rho}\Big\{\rho^2 B_f\sqrt{\pi B_f}\exp\Big(-\frac{B_f\rho^2}{2}\Big)\Big[I_0\Big(\frac{B_f\rho^2}{2}\Big) - I_1\Big(\frac{B_f\rho^2}{2}\Big)\Big]\Big\},$$

where I_m is the modified Bessel function of the first kind of order m, from (24) we obtain

$$T(r, 0, \infty) = A\Lambda\,\frac{\sqrt{\pi B_f}}{2}\,\exp\Big(-\frac{B_f\rho^2}{2}\Big)\Big\{\Big[1 - (1-f)\,\frac{1 - B_f\rho^2}{2}\Big] I_0\Big(\frac{B_f\rho^2}{2}\Big)$$

$$- (1-f)\,\frac{B_f\rho^2}{2}\, I_1\Big(\frac{B_f\rho^2}{2}\Big)\Big\}, \qquad r \geqslant 0. \tag{25}$$

In a similar manner, from (23), we find the temperature distribution along the axis $\rho = 0$:

$$T(0, z, \infty) = A\Lambda\Big\{\frac{Z}{2}\,(1-f) + \Big[\frac{1}{2}\,(1+f) - (1-f)Z^2\Big]\frac{\sqrt{\pi B_f}}{2}\exp\left(B_f Z^2\right)\operatorname{erfc}\left(\sqrt{B_f}Z\right)\Big\}. \tag{26}$$

It follows from Eqs. (25) and (26) that the stationary temperature at the center of the heat-flux source for an arbitrarily distributed intensity of laser radiation (6) is

$$T(0, 0, \infty) = A\Lambda\sqrt{\pi B_f}(1+f)/4. \tag{27}$$

For normally distributed radiation intensity ($f = 1$ and $B_f = 1$), formula (27) yields [22]

$$T(0, 0, \infty) = A\Lambda\sqrt{\pi}/2 \approx 0.8862 A\Lambda,$$

while for the annular distribution ($f = 0$ and $B_f = 2.1462$), we have

$$T(0, 0, \infty) = A\Lambda\sqrt{\pi B_f}/2 \approx 0.6492 A\Lambda.$$

The evolution of the dimensionless temperature $T^* = T/(A\Lambda)$ on the surface at the center of the heat-flux source ($\rho = 0$ and $Z = 0$) and inside the body ($\rho = 0$ and $Z = 0.4$) is illustrated in Fig. 2. It should be noted that the temperature maximum on the body surface corresponds to the end of the laser pulse, $t = t_s$ ($\mathrm{Fo} = \mathrm{Fo}_s$), whereas the temperature maximum in the near-surface layer is observed at the time $t = t_h = t_s + \Delta t$ (in dimensionless variables, we have $\mathrm{Fo}_h = \mathrm{Fo}_s + \Delta\,\mathrm{Fo}$, where $\Delta\,\mathrm{Fo} = k\Delta t/a^2$). As we go father from the working surface of the body, the delay time Δt ($\Delta\,\mathrm{Fo}$) rapidly increases (Fig. 3). At a fixed depth, the delay time Δt has the least value for the normally distributed power density and the highest value for the annular distribution.

The distribution pattern of the power density of incident radiation q^* (18) substantially affects only the surface temperature. The maximum temperature is reached at the center of the heating spot ($r = 0$) in the case of normally distributed radiation intensity and closer to the edge of the spot ($r = 0.6a$) in the case of the annular distribution (Fig. 4). The effective heating depth (distance from the irradiated surface to the point where the temperature amounts to 5% of its maximum value) is almost independent of the distribution of the incident heat-flux intensity, amounting to $1.5a$ for the dimensionless irradiation time $\mathrm{Fo}_s = 0.672$ (Fig. 5).

3. Absorptivity. The delay time Δt is defined as the time at which the temperature T at the point (r, z) inside the body attains its maximum value:

$$\frac{\partial T(r, z, t)}{\partial t}\Big|_{t=t_h} = 0, \qquad r \geqslant 0, \quad z \geqslant 0. \tag{28}$$

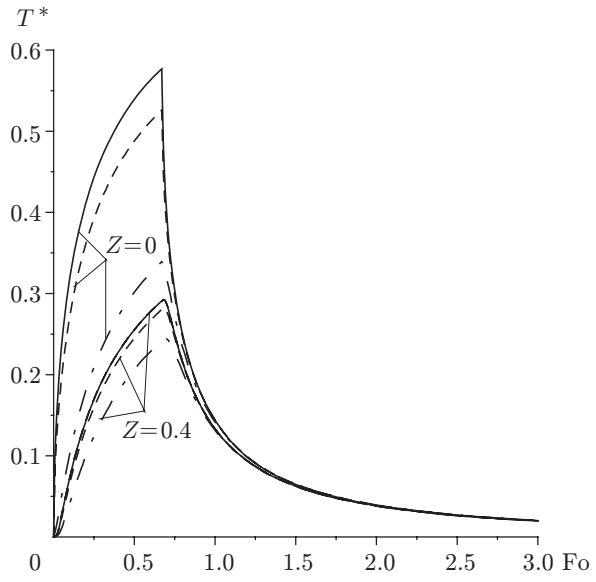

Fig. 2

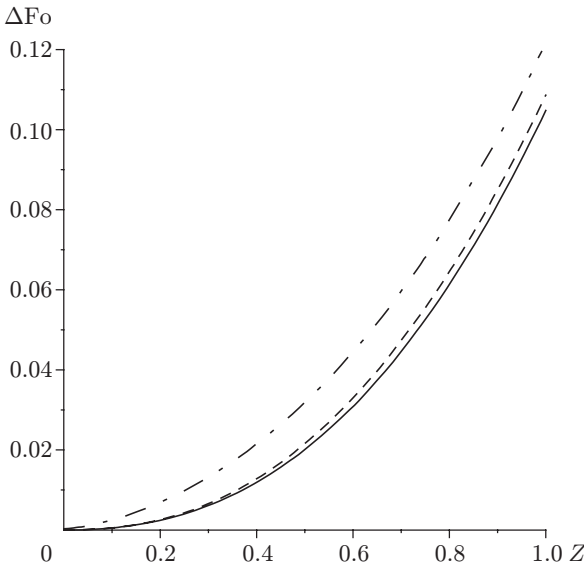

Fig. 3

Fig. 2. Evolution of the dimensionless temperature T^* on the surface of the irradiated body ($\rho = 0$ and $Z = 0$) and inside it ($\rho = 0$ and $Z = 0.4$).

Fig. 3. Distribution of the dimensionless delay time $\Delta\,\mathrm{Fo}$ over the thickness Z of the irradiated body along the axial axis for $\mathrm{Fo} = 0.672$.

We differentiate solution (19)–(22) with respect to the time t and obtain

$$\frac{\partial T(r,z,t)}{\partial t} = A\Lambda\,\frac{æ}{a^2}\,[M(\rho,Z,\mathrm{Fo})H(\mathrm{Fo}) - M(\rho,Z,\mathrm{Fo}-\mathrm{Fo}_s)H(\mathrm{Fo}-\mathrm{Fo}_s)]; \tag{29}$$

$$M(\rho,Z,\mathrm{Fo}) = \int\limits_0^\infty \varphi(\xi)\,\frac{\partial\Phi_0(\xi,Z,\mathrm{Fo})}{\partial\,\mathrm{Fo}}\,J_0(\xi\rho)\,d\xi; \tag{30}$$

$$\frac{\partial\Phi_0(\xi,Z,\mathrm{Fo})}{\partial\,\mathrm{Fo}} = \frac{\xi}{\sqrt{\pi\,\mathrm{Fo}}}\,\exp\Big(-\Big(\frac{Z^2}{4\,\mathrm{Fo}} + \xi^2\,\mathrm{Fo}\Big)\Big). \tag{31}$$

Taking into account the form of the function $\varphi(\xi)$ (20) and the value of derivative (31), we bring the integral $M(\rho,Z,\mathrm{Fo})$ (30) to the form

$$M(\rho,Z,\mathrm{Fo}) = [fM_1(\rho,Z,\mathrm{Fo}) + (1-f)M_2(\rho,Z,\mathrm{Fo})]\exp(-Z^2/(4\,\mathrm{Fo}))/(2\sqrt{\pi\,\mathrm{Fo}}), \tag{32}$$

where, according to [21],

$$M_1(\rho,Z,\mathrm{Fo}) = \int\limits_0^\infty \xi\exp\Big(-\xi^2\Big(\frac{1}{4B_f} + \mathrm{Fo}\Big)\Big)J_0(\xi\rho)\,d\xi = \frac{2B_f}{1+4B_f\,\mathrm{Fo}}\,\exp\Big(-\frac{B_f\rho^2}{1+4B_f\,\mathrm{Fo}}\Big); \tag{33}$$

$$M_2(\rho,Z,\mathrm{Fo}) = \int\limits_0^\infty \Big(1-\frac{\xi^2}{4B_f}\Big)\xi\exp\Big(-\xi^2\Big(\frac{1}{4B_f} + \mathrm{Fo}\Big)\Big)J_0(\xi\rho)\,d\xi$$

$$= \Big[1 - \frac{1}{1+4B_f\,\mathrm{Fo}}\Big(1 - \frac{B_f\rho^2}{1+4B_f\,\mathrm{Fo}}\Big)\Big]M_1(\rho,Z,\mathrm{Fo}). \tag{34}$$

We substitute relations (33) and (34) into equality (32) and obtain

$$M(\rho,Z,\mathrm{Fo}) = \frac{B_f[(1+4B_f\,\mathrm{Fo})(f+4B_f\,\mathrm{Fo}) + (1-f)B_f\rho^2]}{(1+4B_f\,\mathrm{Fo})^3\sqrt{\pi\,\mathrm{Fo}}}\,\exp\Big(-\Big(\frac{B_f\rho^2}{1+4B_f\,\mathrm{Fo}} + \frac{Z^2}{4\,\mathrm{Fo}}\Big)\Big). \tag{35}$$

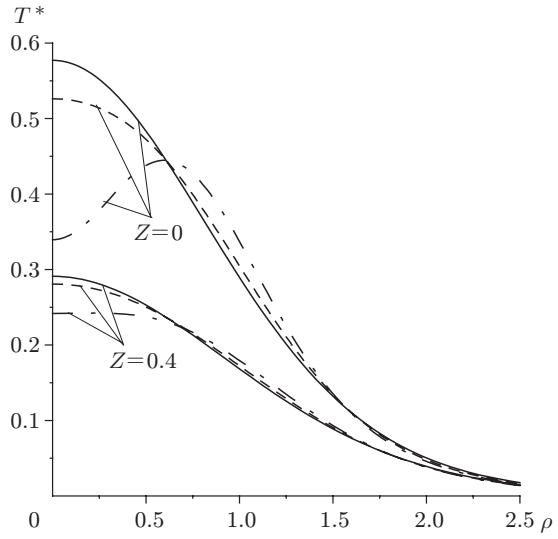

Fig. 4

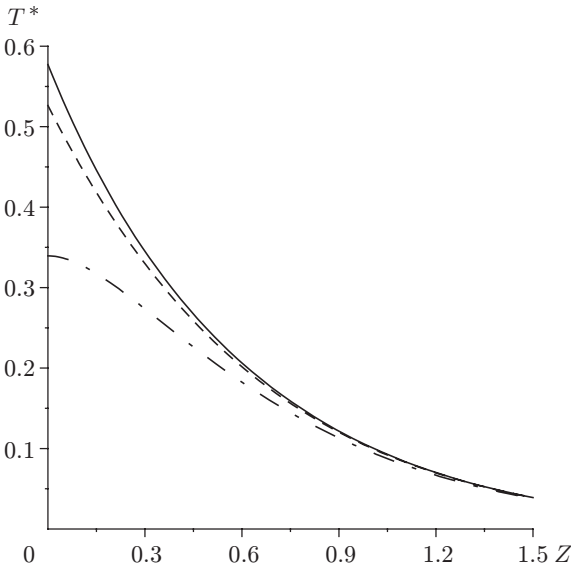

Fig. 5

Fig. 4. Distribution of the dimensionless temperature T^* over the radial coordinate ρ on the half-space surface ($Z = 0$) and at the depth $Z = 0.4$ for $\mathrm{Fo} = 0.672$.

Fig. 5. Variation of the dimensionless temperature T^* over the thickness Z of the irradiated body along the axial axis for $\mathrm{Fo} = 0.672$.

With allowance for relations (29) and (35), condition (28) results in the following nonlinear functional equation for the dimensionless delay time $\Delta\,\mathrm{Fo}$:

$$C_1 C_2^3 D_f(\rho) = \exp\left[-(C_3\rho^2 + C_4 Z^2)\right], \qquad \rho \geqslant 0, \quad Z \geqslant 0. \tag{36}$$

Here

$$C_1 = \sqrt{1 - \frac{\mathrm{Fo}_s}{\mathrm{Fo}_h}}, \qquad C_2 = 1 - \frac{4B_f\,\mathrm{Fo}_s}{1 + 4B_f\,\mathrm{Fo}_h}; \tag{37}$$

$$C_3 = \frac{4B_f\,\mathrm{Fo}_s}{(1 + 4B_f\Delta\,\mathrm{Fo})(1 + 4B_f\,\mathrm{Fo}_h)}, \qquad C_4 = \frac{\mathrm{Fo}_s}{4\Delta\,\mathrm{Fo}\,\mathrm{Fo}_h}; \tag{38}$$

$$D_f(\rho) = \frac{(1-f)B_f\rho^2 + (1 + 4B_f\,\mathrm{Fo}_h)(f + 4B_f\,\mathrm{Fo}_h)}{(1-f)B_f\rho^2 + (1 + 4B_f\Delta\,\mathrm{Fo})(f + 4B_f\Delta\,\mathrm{Fo})}. \tag{39}$$

Taking the logarithm of (36), we obtain

$$C_3\rho^2 + C_4 Z^2 = \ln\left[C_1 C_2^3 D_f(\rho)\right]^{-1}, \qquad \rho \geqslant 0, \quad Z \geqslant 0. \tag{40}$$

Equation (40) defines the temperature-maximum isotherm for given values of Fo_s and $\Delta\,\mathrm{Fo}$ (Fig. 6).

In the case of normally distributed radiation intensity ($f = 1$ and $B_f = 1$), the function $D_f(\rho)$ (39) is independent of the radial variable and equals

$$D_f(\rho) = D_1 = (1 + 4\,\mathrm{Fo}_h)^2/(1 + 4\Delta\,\mathrm{Fo})^2 = C_2^{-2} \tag{41}$$

[the coefficient C_2 is defined by Eq. (37)]. With allowance for (41), Eq. (40) acquires the form

$$\rho^2/\alpha^2 + Z^2/\beta^2 = 1, \qquad |\rho| \leqslant \alpha, \quad 0 \leqslant Z \leqslant \beta, \tag{42}$$

where

$$\alpha^2 = \ln(C_1 C_2)^{-1}/C_3, \qquad \beta^2 = \ln(C_1 C_2)^{-1}/C_4, \tag{43}$$

and the coefficients C_k ($k = 1, 2, 3, 4$) are given by formulas (37) and (38).

Thus, the curve of the maximum dimensionless temperature for the Gaussian distribution of laser power density is a semi-ellipse (42) whose axes are defined by expressions (43) (Fig. 6). The dimensional lengths of the

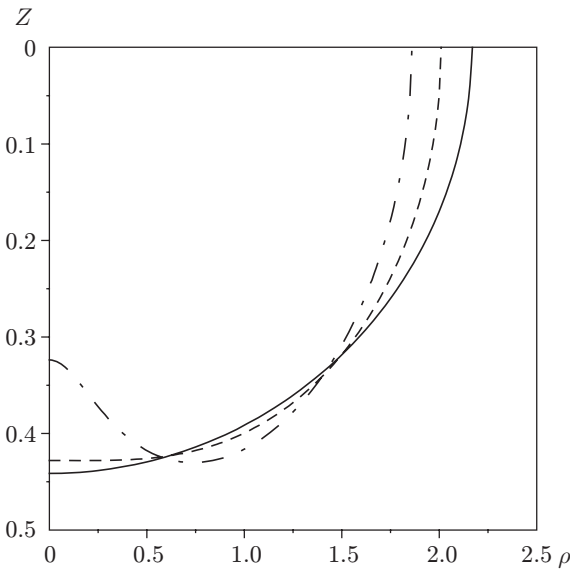

Fig. 6. Curves of maximum dimensional temperature $T^*_{\max}$ calculated for $\mathrm{Fo}_s = 0.672$ and $\Delta\,\mathrm{Fo} = 0.0054$.

axes of this semi-ellipse are $r_h = \alpha a$ and $z_h = \beta a$. In the case of the annular distribution of radiation intensity, the isotherm is shaped as a curve whose maximum is shifted from the axial axis.

Equation (40) can also be considered from an alternative viewpoint. We assume that the shape and size (parameters ρ and Z) of the phase-transformation zone arising in the body when the temperature reaches a certain temperature T_h specific for the body material are known. Then, the dimensionless delay time $\Delta\,\mathrm{Fo}$ can be found from Eq. (40) or (42). After that, the condition $T(r, z, t_h) = T_h$, where the temperature T is given by relations (19)–(22), can be used to derive the final formula for the effective absorptivity:

$$A = T_h A^*/\Lambda. \tag{44}$$

Here

$$A^* = \Big(\int\limits_0^\infty \varphi(\xi)[\Phi_0(\xi, Z, \mathrm{Fo}_s) - \Phi_0(\xi, Z, \Delta\,\mathrm{Fo})] J_0(\xi\rho)\, d\xi \Big)^{-1}. \tag{45}$$

The parameter A^* is plotted in Fig. 7 as a function of the dimensionless delay time $\Delta\,\mathrm{Fo}$ for three distributions of heat-flux density. The calculations were performed by formula (45) for $\rho = 0$ and for the dimensionless depth Z satisfying equality (40).

4. Comparison with Experimental Data. Experimental data for laser-irradiated single-crystal cobalt samples were reported in [23]. Such single crystals are known to have either a hexagonal or a cubic lattice structure. The martensite transition from one phase to the other occurs at $T_h = 693$ K.

The hexagonal phase exhibits strong magnetic anisotropy along the [0001] axis, giving rise to a magnetic field over the plane normal to the anisotropy axis; i.e., in this case, the conditions for the formation of open magnetic domains (regions of the Kittel type) are satisfied. The SEM image of the thus-structured material surface is shown in Fig. 8a. The cubic phase displays open magnetic domains of the Landau–Lifshits type (Fig. 8b).

A single-crystal cobalt sample 5 mm thick was cut so that the microsection of the irradiated surface was orthogonal to the magnetic-anisotropy axis [0001]. Different portions of the sample initially located in air at room temperature were irradiated by pulses from a Kvant-15 laser with a radiation energy $E = 8$ J, pulse duration $t_s = 4.5$ msec, wavelength $\lambda = 1.06$ μm, and heating spot radius $a = 0.35$ mm. The laser power density of the normal (Gaussian) mode was chosen such that only a thin surface layer of the material (thinner than 3 μm) was fused. In this region, and also in the vicinity of this region, no open domains of the Kittel type were observed. After a layer of the sample material approximately 100 μm thick was slowly and carefully ground away, is was possible to observe such domains. Hence, the surface layer was heated at least to the characteristic onset temperature of polymorphic transformations in cobalt, $T_h = 693$ K.

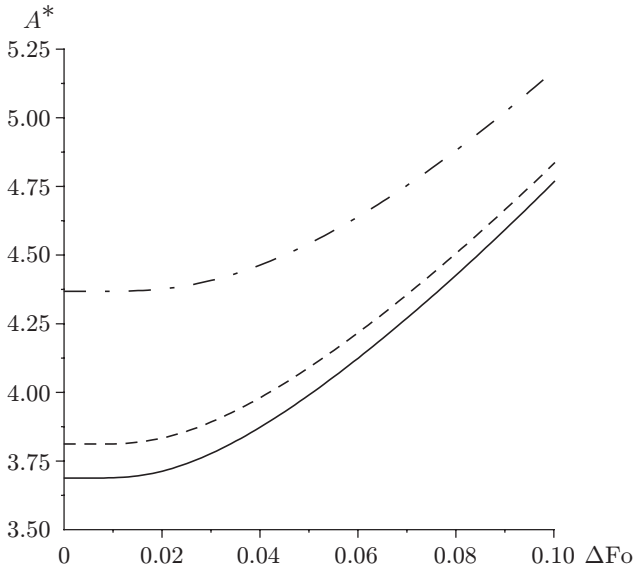

Fig. 7. Parameter A^* versus dimensionless delay time $\Delta\,\mathrm{Fo}$ for $\mathrm{Fo}_s = 0.672$.

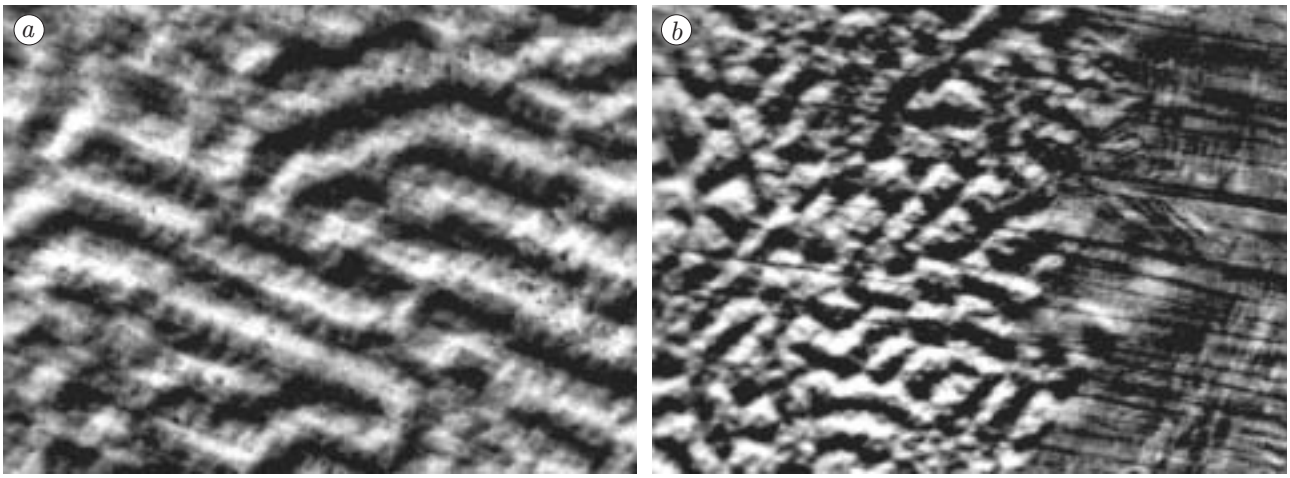

Fig. 8. Laser-irradiated region on the surface of the single-crystal cobalt sample: (a) magnetic-domain structure before radiation; the average width of the domains is 75 μm; (b) magnetic-domain structure after grinding of a 100-μm surface layer.

The thermal conductivity of cobalt is $k = 70.9$ W/(m · K), and its thermal diffusivity is $æ = 1.83{\cdot}10^{-5}$ m^2/sec. The maximum depth of martensite transformations is $z_h \leqslant 100$ μm [23]. The laser power density at the center of the irradiated spot is $q_0 = E/(\pi a^2 t_s) = 4.62 \cdot 10^9$ W/m^2. Thus, we have $\Lambda = 0.228 \cdot 10^5$ K. The dimensionless irradiation time is $\mathrm{Fo}_s = 0.672$, and the maximum dimensionless depth of martensite transformations at the center of the irradiated spot is $Z_h = z_h/a = 0.286$. According to the data in Fig. 3, the dimensionless delay time for these values is $\Delta\,\mathrm{Fo} = 0.0054$. Then, we find $A^* = 3.688$ by formula (45); Eq. (44) yields the effective absorptivity $A = 11.2\%$, which agrees well with the value $A = 10\%$ previously reported by Rożniakowski [3, 23].

Experimental data on laser hardening of St. 45 steel samples [$T_h = 850°$C, $k = 33.5$ W/(m · K), and $æ = 15 \cdot 10^{-6}$ m^2/sec] were reported in [24]. Different portions of the sample shaped as a circular cylinder 6 mm thick and 20 mm in diameter were exposed to pulsed radiation emitted by a glass-based neodymium laser (Nd : YAG) in the standard generation regime ($E = 1.5$ J and $t_s = 2$ msec). After preparation of microsections of the hardened layer and their etching in an alcohol solution of nitric acid, the maximum length (r_h) and depth (z_h) of the hardened zone were measured with the help of an EPITYP-2 metallographic microscope (Fig. 9). The depth of the hardened layer (z_h) was found to be largely dependent on the radiation power density q_0, which could be controlled by focusing.

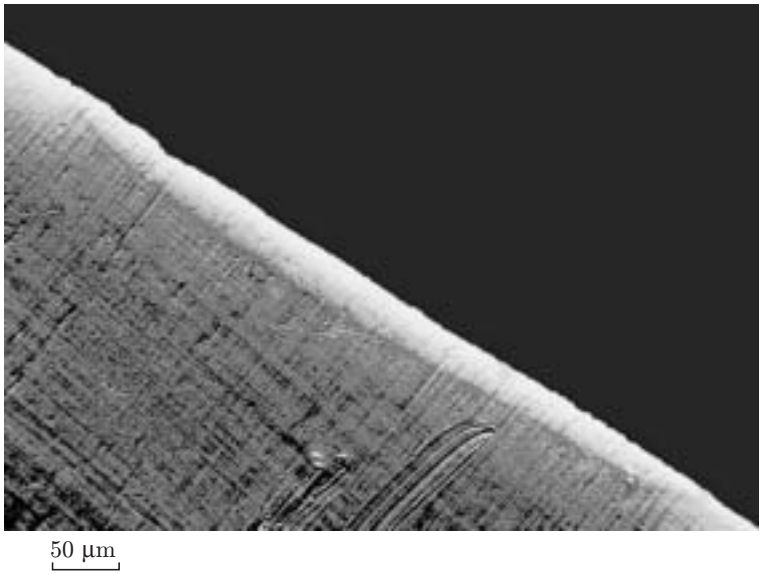

Fig. 9. Region of hardening of the St. 45 steel sample surface.

Fusion of irradiated portions started at $q_0 > 85 \cdot 10^7$ W/m^2. For $q_0 = 58 \cdot 10^7$ W/m^2, the value $z_h = 40$ μm was obtained. The radius of the surface heat-flux source was $a = 0.64$ mm; hence, the dimensionless irradiation duration was $\mathrm{Fo}_s = 0.073$. For $\rho = 0$ and $Z \equiv z_h/a = 0.062$, Eq. (42) yields the dimensionless delay time $\Delta\,\mathrm{Fo} = 0.329 \cdot 10^{-3}$. For these values of dimensionless geometric and time parameters, relation (45) yields $A^* = 4.5$, and formula (44) yields the absorptivity $A = 41.8\%$, which falls within the range of experimental values $A = 30$–50% reported in [24].

Conclusions. In determining the isotherms bounding the phase-transformation region in steel samples, errors in temperature estimates induced by quenching inertia can occur [18]; this circumstance restricts the set of materials to which the method considered in the present paper can be applied. Such materials include metals and metal alloys, for which, first, phase-transition temperatures are known and, second, experimental (laboratory) observations of the onset of structural changes in the metallographic cross section are possible.

REFERENCES

1. N. N. Rykalin, A. A. Uglov, and A. N. Kokora, *Laser Processing of Materials* [in Russian], Mashinostroenie, Moscow (1975).
2. S. I. Anisimov, Ya. A. Imas, G. S. Romanov, and Yu. V. Khodyko, *Effect of High-Intensity Radiation on Metals* [in Russian], Nauka, Moscow (1970).
3. K. Rożniakowski, *Application of Laser Radiation for Examination and Modification of Building Materials Properties*, BIGRAF, Warsaw (2001).
4. A. M. Bonch-Bruevich, Ya. A. Imas, G. S. Romanov, et at., "Variation of metal reflectivity during a laser pulse," *Zh. Tekh. Fiz.*, **38**, No. 5, 851–855 (1968).
5. Kikuo Ujihara, "Reflectivity of metals at high temperatures," *J. Appl. Phys.*, **43**, No. 5, 2376–2383 (1972).
6. I. P. Dobrovol'skii and A. A. Uglov, "Laser heating of solids with allowance for temperature-dependent absorptivity," *Kvant. Electron.*, **1**, No. 6, 1423–1427 (1974).
7. A. V. Bessarab, N. V. Zhidkov, S. B. Korner, et al., "Change in metal-mirror reflectivity under laser radiation," *Kvant. Electron.*, **5**, No. 2, 325–330 (1978).
8. A. I. Korotchenko, A. A. Samokhin, and A. B. Uspenskii, "Behavior of metal absorptivity under laser radiation," *Kvant. Electron.*, **6**, No. 1, 210–217 (1979).
9. V. V. Korneev and A. I. Yavokhin, "Method for analyzing temperature fields and effective absorptivity of metal surfaces treated by a laser beam," *Fiz. Khim. Obrab. Mater.*, No. 2, 7–10 (1980).
10. M. N. Libenson, G. S. Romanov, and Ya. A. Imas, "Laser heating of metals with temperature-dependent optical constants," *Zh. Tekh. Fiz.*, **38**, No. 7, 1116–1119 (1968).

11. A. A. Uglov, I. Yu. Smurov, and A. A. Volkov, "Simulation of metal heating by continuous laser radiation in an oxidizing atmosphere," *Kvant. Electron.*, **10**, No. 2, 289–294 (1983).
12. A. Caruso and C. Strangio, "Space–time structure of the light reflected in an experiment on solid matter irradiation by laser light," *Laser Particle Beams*, **4**, Nos. 3/4, 499–506 (1986).
13. V. S. Velikhikh, V. S. Kartavtsev, A. V. Romanenko, and V. F. Terent'ev, "Impact of laser hardening on mechanical properties of 45 steel samples with different thermal pre-history," *Fiz. Khim. Obrab. Mater.*, No. 2, 12–17 (1984).
14. C.-C. Chen, C.-J. Tao, and L.-T. Shyu, "Eutectoid temperature of carbon steel during laser surface hardening," *J. Mater. Res.*, **11**, No. 2, 458–468 (1996).
15. A. Bokota and S. Iskierka, "Numerical prediction of the hardened zone in laser treatment of carbon steel," *Acta Mater.*, **44**, No. 2, 445–450 (1996).
16. A. Bokota and S. Iskierka, "Effect of phase transformation on stress state in surface layer of laser hardened carbon steel," *ISIJ Int.*, **36**, No. 11, 1383–1391 (1996).
17. R. B. Kuilboer, P.K. Kirner, J. Meijer, et al., "Laser beam transformation hardening: transferability of machining parameters report on a co-operative work in STC'E'," *Ann. CIRP.* **43**, No. 2, 585–592 (1994).
18. V. F. Brekhovskikh, A. N. Kokora, and A. A. Uglov, "Determination of the spatial distribution of the heat-source power in laser-beam-treated steel," *Fiz. Khim. Obrab. Mater.*, No. 6, 3–10 (1967).
19. L. G. Hector and R. B. Hetnarski, "Thermal stresses in materials due to laser heating," in: *Thermal Stresses IV*, Elsevier, Amsterdam (1996), pp. 453–531.
20. A. A. Evtushenko, E. G. Ivanik, S. I. Matysyak, "A model of thermocracking under laser radiation, *Izv. Ross. Akad. Nauk, Mekh. Tverd. Tela*, No. 2, 132–138 (2001).
21. A. P. Prudnikov, Yu. A. Brychkov, and O. I. Marichev, *Integrals and Series. Special Functions* [in Russian], Nauka, Moscow (1983).
22. A. I. Bardybakhin and E. P. Chubarov, "Effect of the shape of the local heat-flux source on the maximum temperature of a thin plate," *Fiz. Khim. Obrab. Mater.*, No. 4, 27–35 (1996).
23. K. Rożniakowski, "Laser-excited magnetic change in cobalt monocrystal," *J. Mater. Sci.*, **26**, 5811–5814 (1991).
24. K. Rożniakowski, S. Vlodarchik, and A. Drobnik, "Determination of temperature of St.45 steel samples under pulsed neodymium-laser radiation," *Kvant. Electron.*, **12**, No. 1, 205–207 (1985).